Schweizerische Eidgenossenschaft
Confédération suisse
Confederazione Svizzera
Confederaziun svizra

Federal Department of the Environment,
Transport, Energy and Communications DETEC

Federal Office of Communications OFCOM
Licences and Frequency Management Division
Radio Technology Section

Ivica Stevanović and Eugenia Cabot, December 8, 2017

OFCOM-Report

The Impact of Body Loss and Transmission Path Loss on Wireless Microphone Radio Links

Executive Summary

In this report, we analyze the effect that body loss and transmission path loss have on wireless microphone radio links. The analyzed cases include scenarios where the wireless microphone transmitter is either body-pack (belt-worn on the back side of the user's body) or hand-held. The main goal of the analysis is to compute the coverage area around the transmitter in which the wireless microphone receiver would have a sufficiently strong reception for a good audio signal quality. The analysis is done over a set of frequencies for which the transmitting antenna gain is obtained from 3-D numerical simulations presented in an earlier study [1]. In our coverage radius simulations, only one receiver antenna is used (no diversity gain) and the transmitter and receiver antennas are at the same height (horizontal plane). Simulations at a higher receiver height have also been performed, but did not provide significantly different results to those obtained assuming the same antenna heights. However, it is to be noted that placing the receiver antenna at a higher position reduces the probability of other people or performers obstructing the direct path between a microphone transmitter and its receiver. Note also that any mismatch of the antenna to the transmitter circuit due to (non)presence of the human body was not taken into account and the simulations always suppose that the entire signal power is transferred to the antenna. Moreover, no interfering signals have been considered in the calculations.

We distinguish two zones around the microphone: the shadow zone in which the wireless microphone link is obstructed by the user's body (in front of the user with a body-pack microphone and behind the user with a hand-held microphone) and the non-shadow zone in which the body does not obstruct the wireless microphone transmission link.

It can be observed that the *gain* of a body-pack or hand-held microphone in the *shadow zone* is smaller than the gain of the corresponding standalone microphone and this difference, that is due to the obstruction of the link by the presence of the body, is significant at all the observed frequencies (235 MHz – 6 GHz). The only exception is in the case of body-pack microphone at lower frequencies, where the wire connecting the microphone with the wireless transmitter acts as a counterpoise (or an extension) to the antenna and allows the signal at those frequencies to be radiated also in the shadow zone. The correlation of the gain with the body size seems to be more pronounced in the case of the hand-held than in the case of the body-pack wireless microphone, the reason for this being in the fact that the body-pack wireless microphone is positioned so much closer to the body that the body size does not play such an important role. The average values of the gain of the body-pack microphone (in the horizontal plane) are for the same reason (the proximity of the body) some 10 dB smaller than the average values of the corresponding case with the hand-held wireless microphone.

On the other hand, the *gain* in the *non-shadow* zone is less affected by the presence of the body than it is the case in the shadow zone. The effect of the user's body in the non-shadow zone is more important at lower frequencies as there is a stronger absorption of the radiated power by the body than it is the case at higher frequencies. Contrary to that, at higher frequencies, the gain of the wireless microphone at

certain directions in the non-shadow zone may even be enhanced in presence of the body as compared to the gain of the corresponding standalone microphone, as at those frequencies the body appears to behave more as a lossy conductor that reflects the radiated energy rather than absorbing it. The values of the gain at lower frequencies are smaller for the body-pack than for the hand-held microphones (due to the closer proximity to the body), and this effect, although in a lesser extent, is also present at higher frequencies as well.

The total body loss for the body-pack microphone has a general trend of decreasing[1] with frequency from about 12 dB at lower simulated frequencies to about 2 dB at the highest one (6 GHz). The same dependence is present in the body loss for the hand-held microphone, with somewhat lower values that range from about 5 dB to about 0.4 dB. Much closer proximity to the body of the body-pack microphone as compared to the hand-held one is the reason for the higher values of the body loss. For the same reason, there does not seem to be a strong correlation of the body size with the body loss values for the body-pack microphone. In the case of the hand-held microphone, this correlation between body loss and size is more apparent.

A cumulative effect of both body loss and transmission loss can be observed in the calculated coverage zones. In general, the coverage of a standalone microphone is always better than the coverage of the same microphone in the presence of the body. It has been observed that the *coverage* in the *shadow zone* of a body-worn microphone (either body-pack or hand-held) is significantly smaller than in the standalone case already at low frequencies and becomes even smaller as the frequency grows. Similarly to the gain, the coverage radius in the shadow zone is correlated with the body size (it appears to be smaller for larger size bodies), noting that this correlation is stronger in the case of the hand-held microphone.

Although the *coverage* in the *non-shadow zone* is larger than 100 m at lower frequencies, it drops down significantly as the frequency grows (due to the predominant effect of the transmission loss compared to the body loss at higher frequencies) making the coverage in the non-shadow zone become practically the same as in the case of a standalone wireless microphone. Furthermore, the coverage radius in the non-shadow zone does not seem to be strongly correlated with the body size.

[1] This frequency dependence has also been observed in the measurements of the body loss for mobile handsets at frequencies 900 MHz and 1800 MHz [2].

Table of Contents

List of Figures

List of Tables

1 Wireless Microphone Radio Link

Referring to Fig. 1, the power of the wireless signal at the PMSE reception can be expressed using the following link budget equation [3]

$$P_{\mathrm{Rx}} = P_{\mathrm{Tx}} + G_{\mathrm{Tx}} - PL - PL_{\mathrm{F}} + G_{\mathrm{Rx}} + G_{\mathrm{D}} \geq P_{\mathrm{Rx,min}}, \tag{1}$$

where

- P_{Tx} [dBm] is the emitted power of the wireless microphone transmitter,
- G_{Tx} [dBi] is the gain of the transmitter antenna in the direction of the receiver including the loss caused by the proximity of the body,
- PL [dB] is the transmission path loss between the transmitter and receiver terminals,
- PL_{F} [dB] is the additional path loss due to multipath and fading effects (causing transmission notches in the received signal),
- G_{Rx} [dBi] is the gain of the receiver antenna in the direction of the transmitter, and
- G_{D} [dB] is the diversity gain (in case more than one antenna is used at the reception).

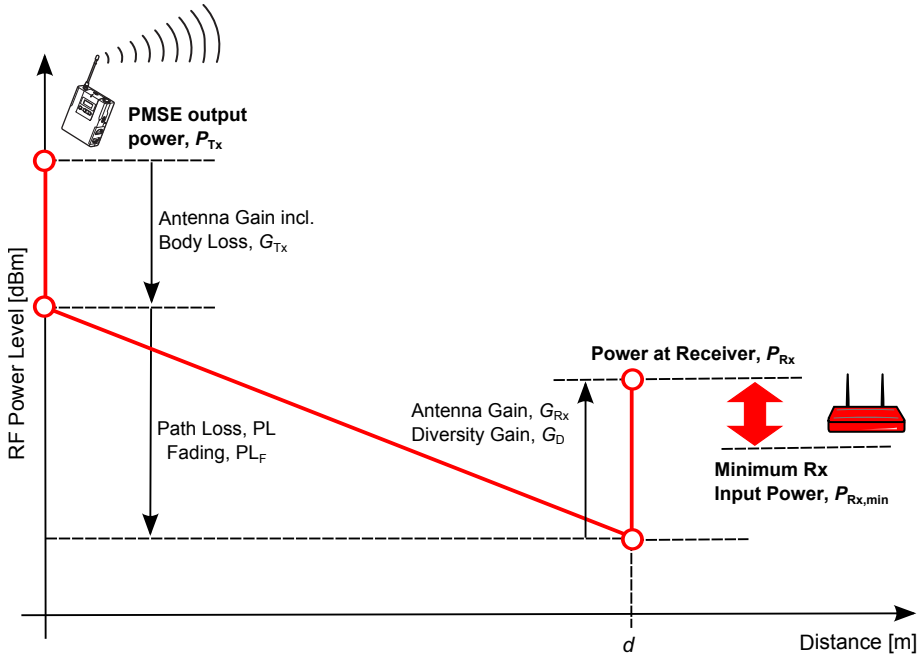

Figure 1: Graphical representation of budget link equation for PMSE radio link.

The RF signal at the input of the receiver unit P_{Rx} [dBm] must not be smaller than the receiver minimum required input signal power $P_{\mathrm{Rx,min}}$ in order to have an acceptable quality of the audio signal at reception.

The path loss was computed supposing a line of sight transmission between the transmitter and receiver and a free-space propagation model that is given by the following equation [3, 4]

$$PL_{\mathrm{dB}} = 32.44 + 10\log_{10}\left(d_{\mathrm{km}}^2 + \frac{(h_{\mathrm{Tx,m}} - h_{\mathrm{Rx,m}})^2}{10^6}\right) + 20\log_{10} f_{\mathrm{MHz}}. \tag{2}$$

The parameters and their corresponding range of values used in the coverage simulations are given in Table 1.

Table 1: The parameters used in the coverage area simulations.

Parameter	Value	Reference
P_{Tx} [dBm]	17	[3]
G_{Tx} [dBi]		[1]
d [m]	1 – 100	
h_{Tx} [m]	1 – 1.5	
h_{Rx} [m]	1 – 4	
f [MHz]	235 – 6000	
PL_F [dB]	30	[3]
G_{Rx} [dBi]	10	[3]
G_D [dB]	0, 7	[3]
$P_{Rx,min}$ [dBm]	–80	[3]

2 Gain Pattern and Coverage of Wireless Microphones

In this section, the gain patterns of both body-pack and hand-held wireless microphones are analyzed when carried or held by three human body models of different sizes and body-mass indices: Eartha (child), Duke (adult male), and Fats (obese adult male). They are taken from [1] and obtained using 3-D full wave numerical simulations in an electromagnetic solver SEMCAD-X. In our coverage radius simulations, only one receiver antenna is used (no diversity gain) and the transmitter and receiver antennas are at the same height. Simulations at a higher receiver height have also been performed, but did not provide significantly different results to those obtained assuming the same antenna heights. However, it is to be noted that placing the receiver antenna at a higher position reduces the probability of other people or performers obstructing the direct path between a microphone transmitter and its receiver. Note also that any mismatch of the antenna to the transmitter circuit due to (non)presence of the human body was not taken into account and the simulations always suppose that the entire signal power is transferred to the antenna. Moreover, no interfering signals have been considered in the calculations.

We distinguish two zones around the microphone: the shadow zone in which the wireless microphone link is obstructed by the body (in front of the presenter with a body-pack microphone and behind the presenter with a hand-held microphone) and the non-shadow zone in which the body does not obstruct the wireless microphone transmission link.

Since the hand-held wireless microphone is positioned with an inclination angle of 45° with respect to the horizontal plane, the gain patterns of the standalone hand-held wireless microphone will not be symmetric in the front and back half-planes, whereas the standalone body-pack microphone is positioned vertically upright and as such will have symmetric gain patterns in those two horizontal half-planes.

Figures 2, 4, and 6 show the gain patterns of a body-pack microphone when carried on body (black lines) and when being standalone (gray lines), whereas Figs. 8, 10, and 12 represent the same gain patterns in the case of a hand-held microphone. It can be observed that the gain of a body-pack or hand-held microphone in the shadow zone is smaller than the gain of the corresponding standalone microphone and this difference (body loss) that is due to the obstruction of the link by the presence of the body is significant at all the observed frequencies. The only exception is in the case of body-pack microphone at lower frequencies, where the wire connecting the microphone with the wireless transmitter acts as a counterpoise (or an extension) to the antenna and allows the signal at those frequencies to be radiated also in the shadow zone. On the other hand, the gain in the non-shadow zone is less affected by the presence of the body than it is the case in the shadow zone. The body loss in the non-shadow zone is more important at lower frequencies as there seem to be a stronger absorption of the radiated power by the body than it is the case at higher frequencies. Contrary to that, the gain of the wireless microphone in the presence of the body at higher frequencies may even be enhanced as compared to the gain of the corresponding standalone microphone as at those frequencies the body seems to behave more as a lossy conductor that reflects the radiated energy rather than absorbing it.

The gain patterns are subsequently used together with the radio link equations presented in Section 1 to calculate a coverage zone around the wireless microphone (in which the received audio signal is of

good quality, $P_{Rx} \geq P_{Rx,min}$, see equation (1)).

Figures. 3, 5, and 7 show the coverage zone around the body-pack microphone, whereas Figs. 9, 11, and 13 represent the coverage zone around the hand-held microphone. Green-colored surface designates the zone in which the received signal is of good audio quality, whereas red-colored surface represents the zone in which there is no reception or the received signal is of poor audio quality. Black lines designate the coverage borderline of the corresponding standalone wireless microphone (i.e., in the absence of the body). In these figures, a cumulative effect of both body loss and transmission loss can be observed. In general, the coverage of a standalone microphone is always larger than the coverage of the same microphone in the presence of the body. It can be seen that the coverage in the shadow zone of a body-worn microphone is significantly smaller than in the standalone case already at low frequencies and becomes even smaller as the frequency grows. Although the coverage in the non-shadow zone is good at lower frequencies, it drops down significantly as the frequency grows (due to the predominant effect of transmission loss at higher frequencies) making the coverage in the non-shadow zones become practically the same as in the case of a standalone wireless microphone.

Tables 2-4 summarize the values of gain and coverage radius around Eartha, Duke, and Fats with the body-pack wireless microphone, whereas Tables 5-7 give the same summary for the hand-held wireless microphone. The values of the gain and coverage radius are shown for the front direction ($\varphi = -90^\circ$) and the back direction ($\varphi = 90^\circ$), together with the average values of the gain and coverage radius in the shadow zone (columns denoted by gray color) and the non-shadow zone. The coverage radius was computed and shown for distances smaller than 100 m and, therefore, if the coverage radius in certain directions is larger than this, only the lower limit is given in the tables. Similarly, for the coverage radii smaller than 3 m, only this upper limit is shown in the tables.

The values of the gain in the shadow zone range from –13 to –36 dBi for the body-pack microphone (in the front direction) and from –3 to –32 dBi for the hand-held microphone (in the back direction). The general tendency is to have lower values of the gain at higher frequencies and for larger bodies, although the values of gain in the front and back directions are highly dependent on the discretization of the azimuth angle and whether the null in the radiation pattern happens to be in those directions. The correlation of the gain with the body size seems to be more pronounced in the case of the hand-held than in the case of the body-pack wireless microphone, the reason for this being in the fact that the body-pack wireless microphone is positioned much closer to the body, reducing thus the impact of the body size. The average values of the gain of the body-pack microphone are for the same reason (the proximity of the body) some 10 dB smaller than the average values of the corresponding case with the hand-held wireless microphone.

Regarding the gain in the non-shadow zone, a trend to increase with frequency is visible in both the gain in the favorable direction and the average gain values. There does not seem to be a strong correlation with the body size. The values of the gain at lower frequencies seem to be smaller for the body-pack than in the case of the hand-held microphones (due to the closer proximity to the body), and this effect, although in a lesser extent, is also present at higher frequencies.

Similarly to the gain, the coverage radius in the shadow zone drops as the frequency increases (mostly due to transmission path loss) and is correlated with the body size (smaller for larger bodies), noting that this correlation is stronger in the case of the hand-held microphone. For the frequencies larger than 1890 MHz, the average values of the coverage radius in the shadow zone are smaller than about 20 m for the body-pack and about 40 m for the hand-held microphone.

In the non-shadow zone, the coverage radius also decreases with frequency but does not seem to be dependent on the body size. For the frequencies larger than 1890 MHz the average values of the coverage radius in the non-shadow zone are smaller than about 60 m for the body-pack and about 80 m for the hand-held microphone.

2.1 Body-Pack Wireless Microphone Worn by a Child

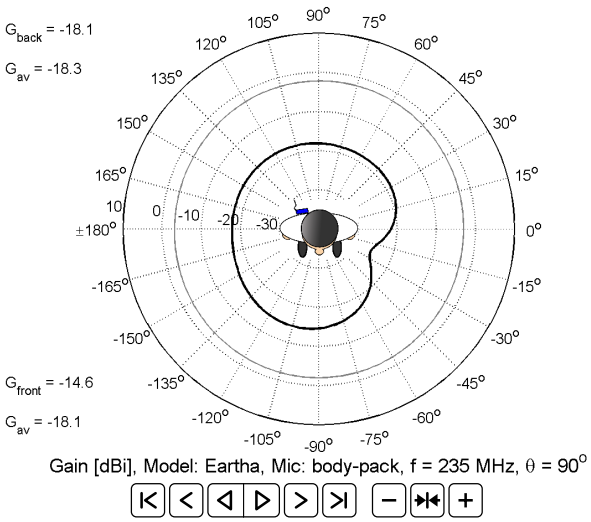

Figure 2: Gain of the stand-alone body-pack wireless transmitter (gray line) and the same transmitter worn by a child (black line). Both transmitter and receiver are assumed to be at the same height. Interactive plot (use the controls to show plots for different frequencies).

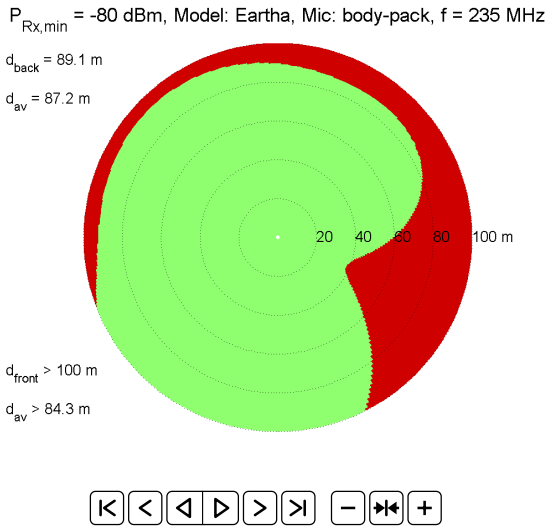

Figure 3: Coverage around the body-pack wireless transmitter worn by a child. Green color depicts the zone where the received signal power is sufficient to provide good audio quality. Black line represents the coverage of the standalone transmitter. Both transmitter and receiver are assumed to be at the same height. Interactive plot (use the controls to show plots for different frequencies).

2.2 Body-Pack Wireless Microphone Worn by an Adult Male

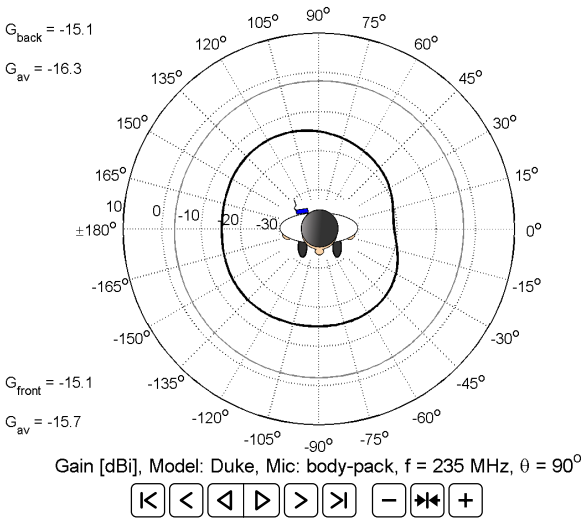

Figure 4: Gain of the stand-alone body-pack wireless transmitter (gray line) and the same transmitter worn by an adult male (black line). Both transmitter and receiver are assumed to be at the same height. Interactive plot (use the controls to show plots for different frequencies).

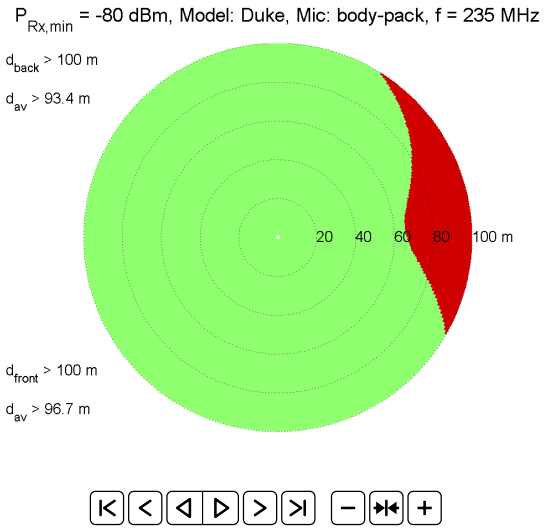

Figure 5: Coverage around the body-pack wireless transmitter worn by an adult male. Green color depicts the zone where the received signal power is sufficient to provide good audio quality. Black line represents the coverage of the standalone transmitter. Both transmitter and receiver are assumed to be at the same height. Interactive plot (use the controls to show plots for different frequencies).

2.3 Body-Pack Wireless Microphone Worn by an Obese Adult Male

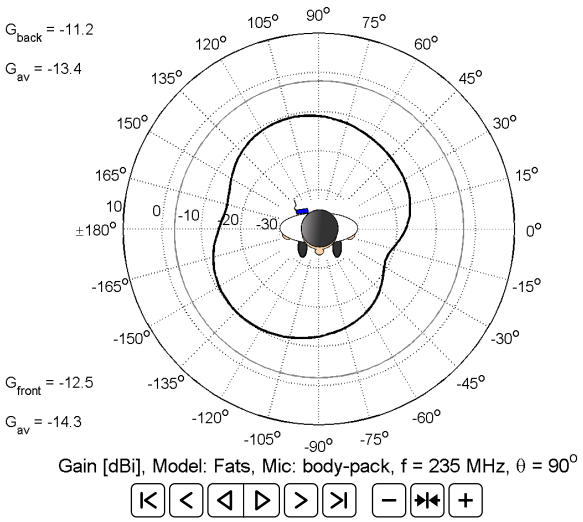

Figure 6: Gain of the stand-alone body-pack wireless transmitter (gray line) and the same transmitter worn by an obese adult male (black line). Both transmitter and receiver are assumed to be at the same height. Interactive plot (use the controls to show plots for different frequencies).

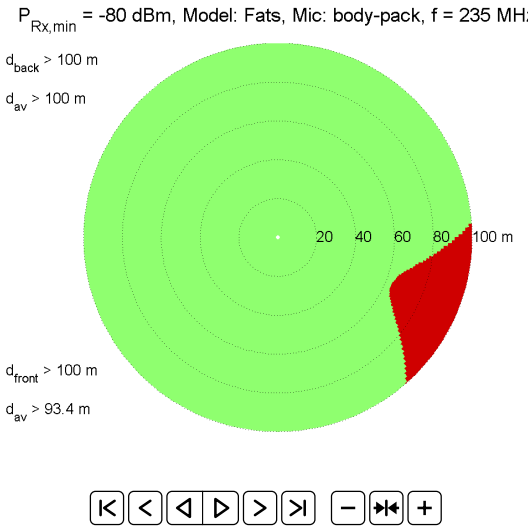

Figure 7: Coverage around the body-pack wireless transmitter worn by an obese adult male. Green color depicts the zone where the received signal power is sufficient to provide good audio quality. Black line represents the coverage of the standalone transmitter. Both transmitter and receiver are assumed to be at the same height. Interactive plot (use the controls to show plots for different frequencies).

2.4 Hand-Held Wireless Microphone Held by a Child

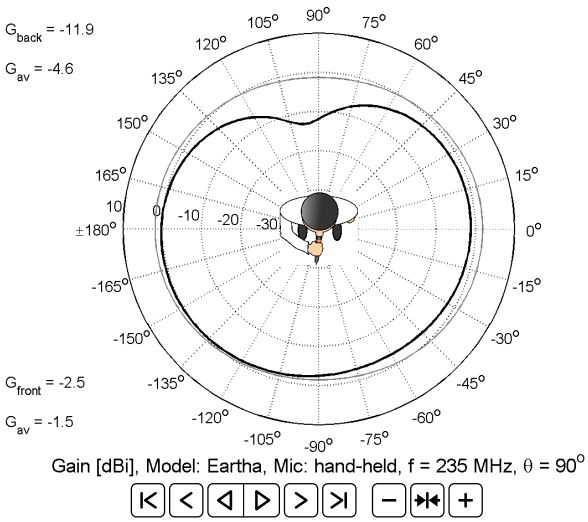

Figure 8: Gain of the stand-alone hand-held wireless transmitter (gray line) and the same transmitter held by a child (black line). Both transmitter and receiver are assumed to be at the same height. Interactive plot (use the controls to show plots for different frequencies).

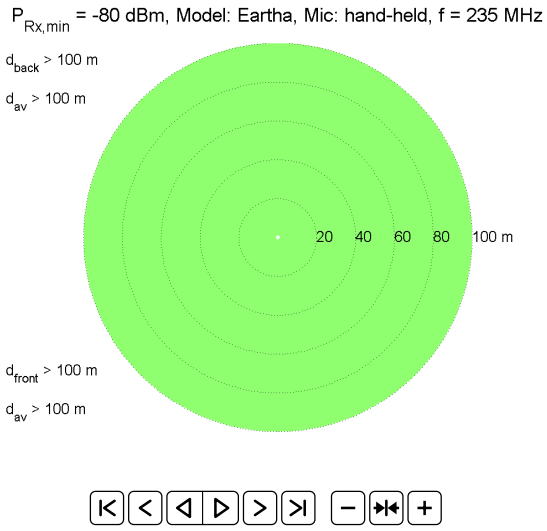

Figure 9: Coverage around the hand-held wireless transmitter held by a child. Green color depicts the zone where the received signal power is sufficient to provide good audio quality. Black line represents the coverage of the standalone transmitter. Both transmitter and receiver are assumed to be at the same height. Interactive plot (use the controls to show plots for different frequencies).

2.5 Hand-Held Wireless Microphone Held by an Adult Male

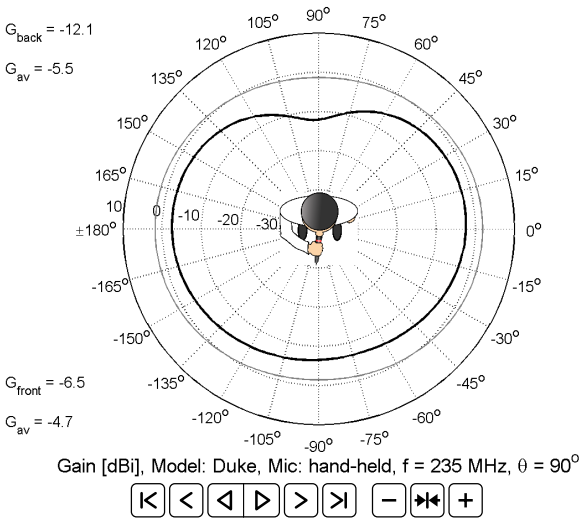

Figure 10: Gain of the stand-alone hand-held wireless transmitter (gray line) and the same transmitter held by an adult male (black line). Both transmitter and receiver are assumed to be at the same height. Interactive plot (use the controls to show plots for different frequencies).

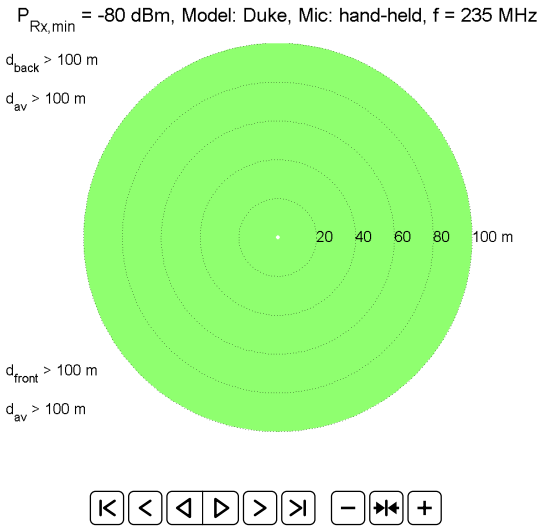

Figure 11: Coverage around the hand-held wireless transmitter held by an adult male. Green color depicts the zone where the received signal power is sufficient to provide good audio quality. Black line represents the coverage of the standalone transmitter. Both transmitter and receiver are assumed to be at the same height. Interactive plot (use the controls to show plots for different frequencies).

2.6 Hand-Held Wireless Microphone Held by an Obese Adult Male

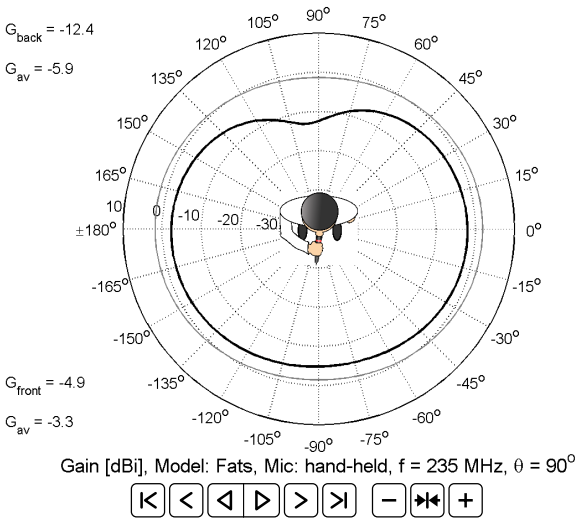

Figure 12: Gain of the stand-alone hand-held wireless transmitter (gray line) and the same transmitter held by an obese adult male (black line). Both transmitter and receiver are assumed to be at the same height. Interactive plot (use the controls to show plots for different frequencies).

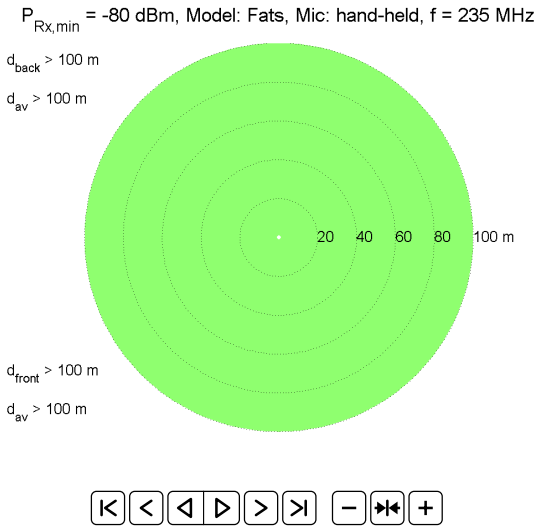

Figure 13: Coverage around the hand-held wireless transmitter held by an obese adult male. Green color depicts the zone where the received signal power is sufficient to provide good audio quality. Black line represents the coverage of the standalone transmitter. Both transmitter and receiver are assumed to be at the same height. Interactive plot (use the controls to show plots for different frequencies).

2.7 Front, Back, and Average Values of Gain and Coverage for Body-Pack Microphone

Table 2: Front, back, and average values of gain and coverage radius in the horizontal plane around Eartha with body-pack wireless microphone. The shadow zone is denoted by gray-colored columns.

f (MHz)	G_{front} (dBi)	G_{av} (dBi)	G_{back} (dBi)	G_{av} (dBi)	d_{front} (m)	d_{av} (m)	d_{back} (m)	d_{av} (m)
235	–14.6	–18.1	–18.1	–18.3	> 100	> 84.3	89.1	87.2
470	–23.4	–14.1	–4.3	–7.8	24.4	> 74.1	> 100	> 97.4
825	–17.2	–15	–3.5	–5.5	27.9	37.8	> 100	> 91.9
1400	–19.4	–17.5	–3	–5.9	12.9	17.3	85.6	66.1
1890	–12.1	–14.3	–1.1	–2.7	21.9	18.4	78.6	67.6
2380	–13.7	–16.7	0.3	–2.7	14.4	11.4	73.6	53.4
3000	–18.4	–19.1	1.5	–3	6.5	6.8	67.2	43.7
3780	–19.6	–19.1	2.2	–0.3	4.5	5.5	57.2	45.6
4760	–25.5	–21.4	0.2	0.4	< 3	3.5	36.3	39.4
6000	–21.3	–21.8	0.9	0.1	< 3	< 3	30.8	29.3

Table 3: Front, back, and average values of gain and coverage radius in the horizontal plane around Duke with body-pack wireless microphone. The shadow zone is denoted by gray-colored columns.

f (MHz)	G_{front} (dBi)	G_{av} (dBi)	G_{back} (dBi)	G_{av} (dBi)	d_{front} (m)	d_{av} (m)	d_{back} (m)	d_{av} (m)
235	–15.1	–15.7	–15.1	–16.3	> 100	> 96.7	> 100	> 93.4
470	–17.9	–15.3	–5.2	–7.6	45.8	64.9	> 100	> 99.1
825	–18.8	–15.5	–1	–3.3	23.4	36.9	> 100	> 96.3
1400	–18.6	–15.9	0.1	–2.9	13.9	21.7	> 100	> 81.8
1890	–13.1	–15.1	0.3	–0.8	19.4	17.8	92.5	> 82.3
2380	–18.1	–18.4	–1.7	–2	8.5	10.1	58.2	57.2
3000	–19	–17.1	2.1	–2.7	6	8.9	72.1	44.5
3780	–26.8	–18.7	2.7	1	< 3	6.5	60.7	52.7
4760	–35.7	–19.4	–1.1	0.8	< 3	4.6	30.8	40.3
6000	–27.4	–21.8	–3.7	–0.7	< 3	3.3	17.9	26.5

Table 4: Front, back, and average values of gain and coverage radius in the horizontal plane around Fats with body-pack wireless microphone. The shadow zone is denoted by gray-colored columns.

f (MHz)	G_{front} (dBi)	G_{av} (dBi)	G_{back} (dBi)	G_{av} (dBi)	d_{front} (m)	d_{av} (m)	d_{back} (m)	d_{av} (m)
235	–12.5	–14.3	–11.2	–13.4	> 100	> 93.4	> 100	> 100
470	–18.3	–17.8	–7.5	–9.2	43.3	47.6	> 100	> 96.1
825	–20.1	–22	–5.2	–8.3	19.9	17.9	> 100	> 80.4
1400	–20.3	–20.1	–0.1	–4.6	11.4	13.4	> 100	> 73.4
1890	–21	–19.9	–1.1	–2.8	7.5	10.4	78.6	> 67.7
2380	–20.9	–22.8	–1.8	–3.7	6	5.9	57.2	48.6
3000	–23	–20.6	1.6	–3.8	4	5.6	67.7	40.6
3780	–26.1	–22.5	3.2	0.3	< 3	3.8	64.2	50.2
4760	–25.6	–24	0.5	0.2	< 3	< 3	37.3	38.8
6000	–27.2	–26	1.1	–0.1	< 3	< 3	31.3	29.1

2.8 Front, Back, and Average Values of Gain and Coverage for Hand-Held Microphone

Table 5: Front, back, and average values of gain and coverage radius in the horizontal plane around Eartha with hand-held wireless microphone. The shadow zone is denoted by gray-colored columns.

f (MHz)	G_{front} (dBi)	G_{av} (dBi)	G_{back} (dBi)	G_{av} (dBi)	d_{front} (m)	d_{av} (m)	d_{back} (m)	d_{av} (m)
235	–2.5	–1.5	–11.9	–4.6	> 100	> 100	> 100	> 100
470	–3.5	–2	–7.3	–2.6	> 100	> 100	> 100	> 98.3
825	–6.7	–6.2	–2.9	–5.7	67.2	> 71.5	> 100	> 76.8
1400	–5.6	–2.9	–8.6	–5.4	44.8	63.7	31.8	50.6
1890	–6.1	–3.7	–9.3	–4.8	31.3	42.4	21.4	42
2380	–0.5	–1.3	–10.8	–6.3	46.8	43.7	14.4	29.1
3000	–3.3	–1	–11.1	–5.9	26.9	36.7	10.9	24.1
3780	1.7	1.2	–15.7	–6.7	38.3	36.3	5	18
4760	3	1.4	–14.3	–9.3	35.3	29.7	4.5	10.7
6000	5.4	1.5	–15.7	–8.9	36.8	24.8	3	8.3

Table 6: Front, back, and average values of gain and coverage radius in the horizontal plane around Duke with hand-held wireless microphone. The shadow zone is denoted by gray-colored columns.

f (MHz)	G_{front} (dBi)	G_{av} (dBi)	G_{back} (dBi)	G_{av} (dBi)	d_{front} (m)	d_{av} (m)	d_{back} (m)	d_{av} (m)
235	–6.5	–4.7	–12.1	–5.5	> 100	> 100	> 100	> 100
470	–6.3	–6.7	–8.2	–3.6	> 100	> 96.5	99	> 99.9
825	–10.6	–5.9	–6.1	–5.6	42.8	> 73.5	71.6	> 75.5
1400	–12.4	–4.3	–13	–6.9	20.4	57.6	18.9	44.8
1890	–0.3	–1	–24.3	–6.6	61.2	57	3.5	38.1
2380	–8.3	–3.1	–19.7	–6.4	18.9	38.1	5	30.1
3000	–1.5	–0.4	–17.9	–7	33.3	38.2	5	23.1
3780	–3.4	0.3	–18.2	–8.2	21.4	33	3.5	16.5
4760	3.2	1.1	–17.6	–10.9	36.3	29	3	9.3
6000	1.6	1	–21	–11.2	23.9	23.5	< 3	7.3

Table 7: Front, back, and average values of gain and coverage radius in the horizontal plane around Fats with hand-held wireless microphone. The shadow zone is denoted by gray-colored columns.

f (MHz)	G_{front} (dBi)	G_{av} (dBi)	G_{back} (dBi)	G_{av} (dBi)	d_{front} (m)	d_{av} (m)	d_{back} (m)	d_{av} (m)
235	–4.9	–3.3	–12.4	–5.9	> 100	> 100	> 100	> 100
470	–6.6	–6	–10.3	–5.8	> 100	> 100	77.1	> 95.8
825	–4.1	–2.8	–10.2	–8.6	90.1	> 96.7	44.8	55.9
1400	–1.3	–2.1	–18	–10.4	73.6	> 68.5	10.5	> 35.2
1890	–4.5	–0.9	–28.1	–9.3	37.3	58.2	< 3	31
2380	–2.3	–2.8	–23.3	–9	38.3	39.2	3	26.2
3000	–6.9	–1.7	–21.4	–9.3	17.9	35	3	19.7
3780	0.1	1.2	–32.3	–10.8	31.8	36.7	< 3	14.4
4760	3.5	1.9	–19.2	–12.2	37.3	31.8	< 3	9.2
6000	3.7	1.3	–30.2	–14.3	30.4	24.3	< 3	5.1

2.9 The Impact of Receiving Antenna Diversity on Coverage

In the simulations presented hitherto, we have assumed that there is no antenna diversity at reception ($G_D = 0$ in (1)). In this section, we analyze the case when antenna diversity techniques are used to increase the gain at the receiving end by $G_D > 0$.

Let d_1 be the coverage distance in a given direction around a wireless microphone when there is no diversity at the receiver and d_2 the coverage distance of the same microphone in the same direction when there is diversity at reception. From the link budget equation (1) we obtain for these two cases, considering all the other parameters being equal:

$$P_{Rx,min} = P_{Tx} + G_{Tx} - PL(d_1) - PL_F + G_{Rx}$$

$$P_{Rx,min} = P_{Tx} + G_{Tx} - PL(d_2) - PL_F + G_{Rx} + G_D$$

which further yields

$$PL(d_2) - PL(d_1) = G_D.$$

Considering the free space (LoS) path loss and assuming that both transmitter and receiver antennas are at the same height, the relation between the coverage distances with and without the diversity at the reception becomes

$$d_2 = d_1 \cdot 10^{\frac{G_D}{20}}.$$

For the value of diversity gain of $G_D = 7$ dB [3], this would mean that the coverage distance is $10^{\frac{7}{20}} \approx 2.2$ times as large as the coverage distance when no diversity techniques are applied.

3 Body Loss of Wireless Microphones

As shown in previous sections, the gain of wireless microphones (i.e., the radiated power) in a proximity of a user’s body is generally reduced when compared to the case when the wireless microphone operates in free space (without presence of the user). The body loss (BL) can be defined as the ratio of the radiated power with and without the user’s body and its effect on radiation is twofold [2]:

- the presence of a human tissue near the wireless microphone antenna changes the input impedance of the antenna, which may either improve or degrade the antenna matching, thus changing the amount of radiated power
- one part of the radiated power is absorbed in the human tissue leading to reduced radiation efficiency

According to the definition, the body loss can be expressed as

$$BL = -10 \log_{10} \frac{p_{\text{rad}}}{p_{\text{rad,fs}}}$$

where p_{rad} and $p_{\text{rad,fs}}$ are radiated powers with and without the user’s body, respectively:

$$p_{\text{rad}} = \frac{p_{\text{Tx}}}{4\pi} \int_{\varphi} \int_{\theta} g(\varphi, \theta) \sin\theta \, \mathrm{d}\theta \, \mathrm{d}\varphi$$

$$p_{\text{rad,fs}} = \frac{p_{\text{Tx}}}{4\pi} \int_{\varphi} \int_{\theta} g_{\text{fs}}(\varphi, \theta) \sin\theta \, \mathrm{d}\theta \, \mathrm{d}\varphi$$

In the above equations p_{Tx} is the power supplied to the antenna and $g(\varphi, \theta)$ and $g_{\text{fs}}(\varphi, \theta)$ are the gain of the antenna (in linear scale) with and without the user, respectively.

Note that the effect of antenna mismatch was not taken into account in our study. The measured antenna mismatch in hand-held mobile phones in talk position was less than 2 dB of the total body loss as shown in [5].

Using this formulation, we computed the total body loss for body-pack and hand-held wireless microphones in the presence of three different users (Eartha, Duke, and Fats), as well as the parts of body loss as pertaining to the the semi-spaces in front of and behind the user.

Figures 14, 15, and 16 show the gain patterns of the body-pack microphone when carried on body (left) and when being standalone (right), as a function of the azumuth $\varphi \in [0^\circ, 360^\circ]$ and elevation angles $\theta \in [0^\circ, 180^\circ]$, and frequency. The body loss values computed using the gain patterns are also shown in these figures and summarized in Table 8. Similarly, Figs. 17, 18, 19 and Table 9 represent the same gain patterns and body loss values in the case of the hand-held microphone.

It can be observed that the total body loss for the body-pack microphone has a general trend of decreasing with frequency from about 12 dB at the lowest frequency to about 2 dB at the highest one. The same can be observed in the body loss for the hand-held microphone, with somewhat lower values that range from about 5 dB to about 0.4 dB. Much closer proximity to the body of the body-pack microphone as compared to the hand-held one is the reason for the higher values of the body loss. For the same reason, there does not seem to be a strong correlation of the body size with the body loss values for the body-pack microphone. In the case of the hand-held microphone, this correlation is more apparent.

3.1 Body Loss for Body-Pack Wireless Microphone Worn by a Child

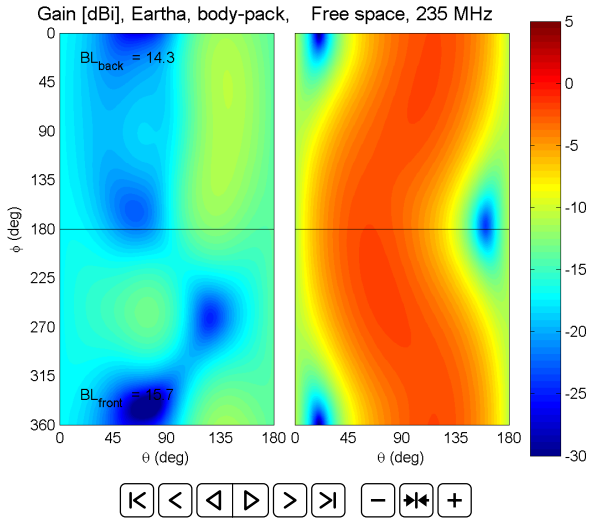

Figure 14: Gain of the body-pack wireless transmitter worn by a child (left) and of a standalone transmitter (right) as a function of azimuth φ and elevation θ angles. Horizontal line depicts the border between the semi-spaces in front of and behind the user. The body loss values are computed using the stand alone body-pack wireless transmitter as a reference. Interactive plot (use the controls to show plots for different frequencies).

3.2 Body Loss for Body-Pack Wireless Microphone Worn by an Adult Male

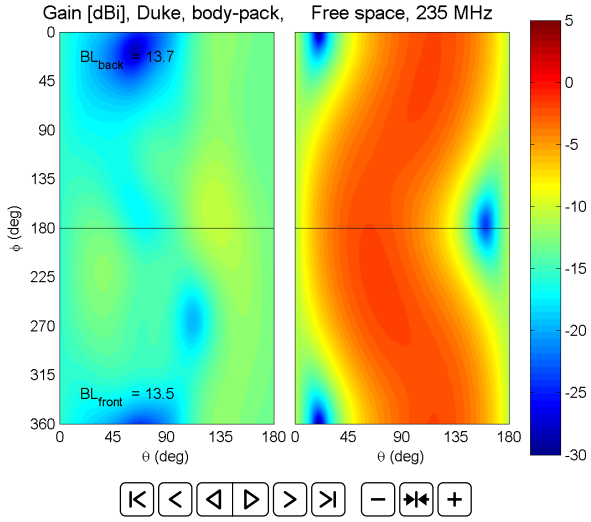

Figure 15: Gain of the body-pack wireless transmitter worn by an adult male (left) and of a standalone transmitter (right) as a function of azimuth φ and elevation θ angles. Horizontal line depicts the border between the semi-spaces in front of and behind the user. The body loss values are computed using the stand alone body-pack wireless transmitter as a reference. Interactive plot (use the controls to show plots for different frequencies).

3.3 Body Loss for Body-Pack Wireless Microphone Worn by an Obese Adult Male

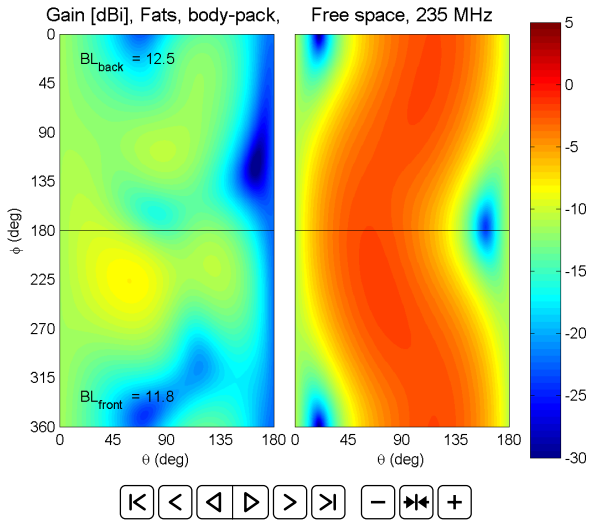

Figure 16: Gain of the body-pack wireless transmitter worn by an obese adult male (left) and of a standalone transmitter (right) as a function of azimuth φ and elevation θ angles. Horizontal line depicts the border between the semi-spaces in front of and behind the user. The body loss values are computed using the stand alone body-pack wireless transmitter as a reference. Interactive plot (use the controls to show plots for different frequencies).

3.4 Body Loss for Hand-Held Wireless Microphone Held by a Child

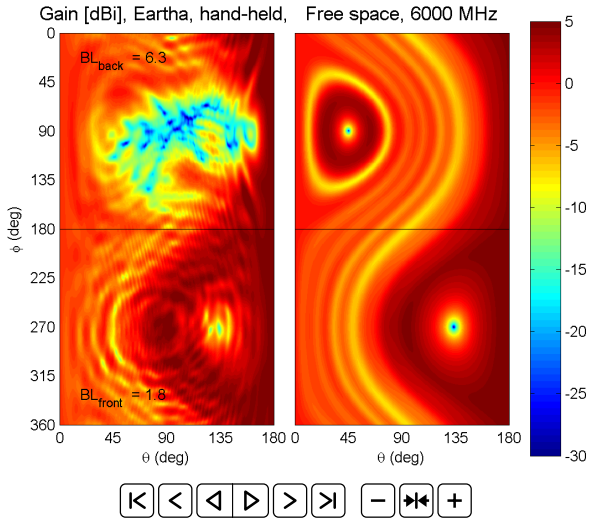

Figure 17: Gain of the hand-held wireless transmitter held by a child (left) and of a standalone transmitter (right) as a function of azimuth φ and elevation θ angles. Horizontal line depicts the border between the semi-spaces in front of and behind the user. The body loss values are computed using the stand alone hand-held wireless transmitter as a reference. Interactive plot (use the controls to show plots for different frequencies).

3.5 Body Loss for Hand-Held Wireless Microphone Held by an Adult Male

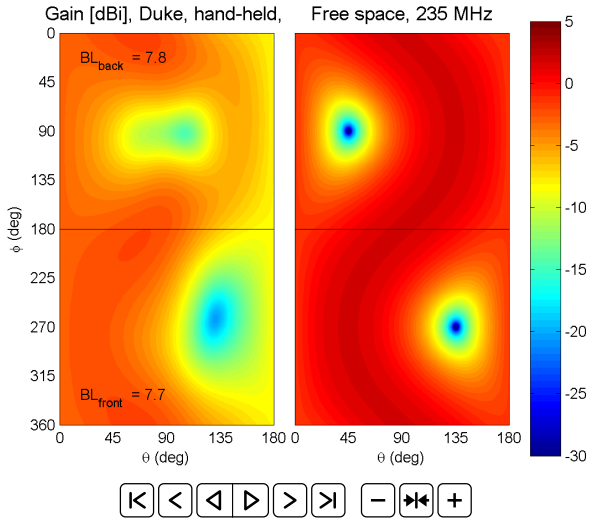

Figure 18: Gain of the hand-held wireless transmitter held by an adult male (left) and of a standalone transmitter (right) as a function of azimuth φ and elevation θ angles. Horizontal line depicts the border between the semi-spaces in front of and behind the user. The body loss values are computed using the stand alone hand-held wireless transmitter as a reference. Interactive plot (use the controls to show plots for different frequencies).

3.6 Body Loss for Hand-Held Wireless Microphone Held by an Obese Adult Male

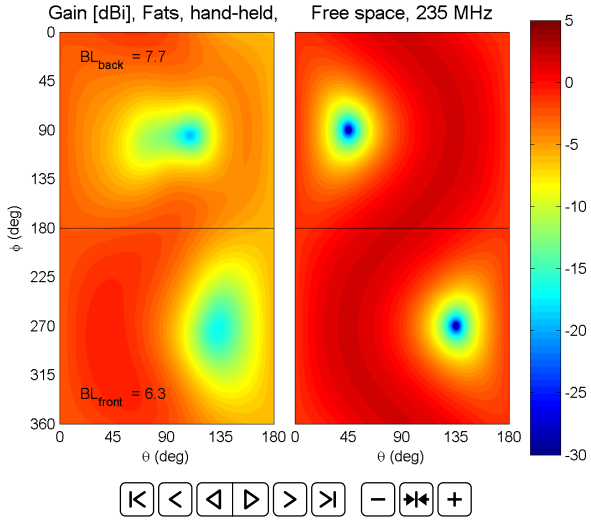

Figure 19: Gain of the hand-held wireless transmitter held by an obese adult male (left) and of a standalone transmitter (right) as a function of azimuth φ and elevation θ angles. Horizontal line depicts the border between the semi-spaces in front of and behind the user. The body loss values are computed using the stand alone hand-held wireless transmitter as a reference. Interactive plot (use the controls to show plots for different frequencies).

3.7 Summary of Body Loss Values

Table 8: Total body loss and body loss in the semi-spaces in front of and behind a human model with body-pack wireless microphone. The shadow zone is denoted by gray-colored columns.

	Eartha			Duke			Fats		
f (MHz)	BL_{fr}	BL_{bck}	BL_{tot}	BL_{fr}	BL_{bck}	BL_{tot}	BL_{fr}	BL_{bck}	BL_{tot}
235	15.7	14.3	11.9	13.5	13.7	10.5	11.8	12.5	9.1
470	15.7	10.9	9.6	16.7	11	10	19.2	12.4	11.6
825	16.2	9.5	8.7	16.9	7.7	7.2	22.2	12	11.6
945	16.5	9.1	8.4	16.6	6.7	6.3	22.1	11.2	10.9
1400	18.5	9	8.6	16.6	6.3	5.9	20.6	7.8	7.6
1890	16.4	5.9	5.5	15.6	4.4	4.1	19.4	5.4	5.2
2380	16.6	4.8	4.5	16.8	3.7	3.5	19.7	4.4	4.2
3000	16.9	3.5	3.3	16.3	2.5	2.4	18.8	3.1	3
3780	16.5	2.4	2.3	17	1.7	1.6	18.8	2.2	2.1
4760	17.4	2.2	2.1	17.1	1.8	1.7	19.1	2.1	2
6000	17.4	2	1.9	16.5	1.9	1.8	19	1.9	1.8

Table 9: Total body loss and body loss in the semi-spaces in front of and behind a human model with hand-held wireless microphone. The shadow zone is denoted by gray-colored columns.

	Eartha			Duke			Fats		
f (MHz)	BL_{fr}	BL_{bck}	BL_{tot}	BL_{fr}	BL_{bck}	BL_{tot}	BL_{fr}	BL_{bck}	BL_{tot}
235	4.9	6.4	2.6	7.7	7.8	4.7	6.3	7.7	4
470	4.2	5.5	1.8	7.1	6	3.5	6.9	7.4	4.1
825	6.9	5.4	3.1	7.5	5.8	3.6	5.6	7.6	3.5
945	7	5.2	3	8.1	5.8	3.8	6	7.9	3.8
1400	5.5	5.3	2.4	6.2	6.5	3.4	4.5	8.8	3.1
1890	5	5.3	2.2	5	6	2.5	4	7.4	2.4
2380	4.1	5.3	1.6	4.8	6	2.4	4	6.8	2.2
3000	3.6	4.9	1.2	3.7	5.9	1.6	3.6	6.6	1.8
3780	2.7	5.1	0.7	2.9	6.3	1.2	2.6	7.2	1.3
4760	2.4	5.6	0.7	2.4	6.7	1	2.3	7.5	1.1
6000	1.8	6.3	0.5	1.8	7.5	0.7	1.8	8.2	0.9

References

[1] E. Cabot and M. H. Capstick, “The effect of the human body on wireless microphone transmission,” IT’IS Foundation, Zurich, Tech. Rep. July, 2015. [Online]. Available: https://www.bakom.admin.ch/dam/bakom/en/dokumente/frequenzen/report_the_effectofthehumanbodyonwirelessmicrophonetransmission.pdf

[2] J. Krogerus, J. Toivanen, C. Icheln, and P. Vainikainen, “Effect of the human body on total radiated power and the 3-D radiation pattern of mobile handsets,” *IEEE Transactions on Instrumentation and Measurement*, vol. 56, no. 6, pp. 2375–2385, 2007.

[3] ETSI, *Electromagnetic compatibility and Radio spectrum Matters (ERM); Technical characteristics for Professional Wireless Microphone Systems (PWMS); System Reference Document (TR 102 546 - V1.1.1)*, European Telecommunications Standards Institute, 2005. [Online]. Available: http://www.etsi.org/deliver/etsi_tr/102500_102599/102546/01.01.01_60/tr_102546v010101p.pdf

[4] ITU, *ITU-R Recommendation P.525-2: Calculation of Free-space Attenuation*, International Telecommunications Union, Aug. 1994. [Online]. Available: http://www.itu.int/rec/R-REC-P.525/en

[5] G. F. Pedersen, K. Olesen, and S. L. Larsen, “Antenna efficiency of handheld phones,” in *IEE Seminar on Electromagnetic Assessment and Antenna Design Relating To Health Implications of Mobile Phones*, June 1999, pp. 6/1–6/5.

Revision History

Revision	Date	Author(s)	Description
1.0	23.09.2016	I. Stevanović	Initial Draft
1.1	24.10.2016	I. Stevanović	Introduced comments from E. Cabot
1.2	25.10.2016	I. Stevanović	Introduced Section 2.9 as suggested by D. Vergères
1.3	04.07.2017	I. Stevanović and E. Cabot	Adjusted colorbars in Section 3
1.4	08.12.2017	I. Stevanović	Corrected equations and body loss values in Section 3